The microtubule catastrophe promoter Sentin delays stable kinetochore-microtubule attachment in oocytes

#201507006 Revison

The microtubule catastrophe promoter Sentin delays stable kinetochore-microtubule attachment in oocytes

A. Agata Głuszek[1,6], C. Fiona Cullen[1,6], Wenjing Li[2,4,6], Rachel A. Battaglia[3,5], Sarah J. Radford[3], Mariana F. Costa[1], Kim S. McKim[3], Gohta Goshima[2] and Hiroyuki Ohkura[1,7]

(1) Wellcome Trust Centre for Cell Biology, School of Biological Sciences, The University of Edinburgh, EH9 3BF, UK

(2) Division of Biological Science, Graduate School of Science, Nagoya University, Furo-cho, Chikusa-ku, Nagoya 464-8602, Japan

(3) Waksman Institute, Rutgers, the State University of New Jersey, Piscataway, NJ 08854

(4) Present address: Tsinghua-Peking Center for Life Sciences, School of Life Sciences, Tsinghua University, Beijing 100084, China

(5) Present address: University of North Carolina, Biological and Biomedical Sciences Program, Chapel Hill, NC 27599

(6) These authors contribute equally

(7) Corresponding author: h.ohkura@ed.ac.uk, +44-131-650-7094

eTOC summary: Microtubule plus ends are actively prevented from forming stable attachment to kinetochores during spindle formation in *Drosophila* oocytes. The microtubule catastrophe-promoting complex Sentin-EB1 is responsible for this delay in attachment, and facilitates bipolar attachment of homologous chromosomes.

22,324 characters

Abstract

The critical step in meiosis is to attach homologous chromosomes to the opposite poles. In mouse oocytes, stable microtubule end-on attachments to kinetochores are not established until hours after spindle assembly, and phosphorylation of kinetochore proteins by Aurora B/C is responsible for the delay. Here we demonstrated that microtubule ends are actively prevented from stable attachment to kinetochores until well after spindle formation in *Drosophila* oocytes. We identified the microtubule catastrophe-promoting complex Sentin-EB1 as a major factor responsible for this delay. Without this activity, microtubule ends precociously form robust attachments to kinetochores in oocytes, leading to a high proportion of homologous kinetochores stably attached to the same pole. Therefore, regulation of microtubule ends provides an alternative novel mechanism to delay stable kinetochore-microtubule attachment in oocytes.

Introduction

Meiosis is a special cell division that differs from mitosis in many aspects. The key event is to establish stable bipolar attachment of homologous chromosomes. For more than a decade, it has been known in mouse oocytes that stable attachments of microtubule ends to kinetochores are not established for hours after nuclear envelope breakdown (Brunet et al, 1999). This delay is likely to help prevent incorrect attachment before the formation of a bipolar spindle which requires several hours due to lack of centrosomes. This process was studied at a higher resolution, revealing that each kinetochore undergoes multiple bi-orientation attempts before stable bipolar attachment (Kitajima et al, 2011). It was shown that a slow increase of Cdk1 activity in oocytes delays kinetochore-microtubule attachments (Davydenko et al., 2013). Most recently, it was shown that phosphorylation of kinetochore proteins by Aurora B/C is responsible for this delay and gradual increase of the Cdk1 activity induces PP2A-B56 recruitment to kinetochores to stabilise the attachments (Yoshida et al., 2015). Therefore, phospho-regulation of kinetochore proteins is a key mechanism to delay stable attachment in mouse oocytes.

Fine-tuning of kinetochore-microtubule attachment requires precise control of microtubule plus end dynamics as well as regulation of kinetochore proteins. In recent years, great advances have been made in understanding how the kinetochore complex is assembled and interacts with dynamic microtubule ends (Cheeseman, 2014). In contrast, less attention has been paid to regulation of microtubule ends. One of the critical regulators of microtubule plus ends is the conserved protein EB1, which can track growing microtubule plus ends and recruits many microtubule regulators to plus ends.

Sentin (also known as Ssp2; Goshima et al., 2007) was shown to be a major EB1 effector in a *Drosophila* S2 cell line (Li et al., 2011). Sentin is recruited to microtubule plus ends by EB1, and its depletion increases microtubule pausing in cultured cells (Li et al., 2011). Sentin also enhances the association of the microtubule polymerase Mini spindles

(Msps), the XMAP215 orthologue, to microtubule plus ends. These properties are shared with mammalian SLAIN2 (van der Vaart et al., 2011), a potential functional homologue of Sentin. *In vitro* reconstitution from pure proteins demonstrated that Sentin, together with EB1, increases the microtubule growth rate and catastrophe frequency (Li et al., 2012). Additionally, in combination with Msps, the Sentin-EB1 complex synergistically increases microtubule growth rates, and also promotes rescue. The importance of Sentin in microtubule regulation was shown in S2 cells and *in vitro*, but Sentin has not previously been studied in a whole organism.

In this report, we examined the role of Sentin in *Drosophila* oocytes. Little is known in *Drosophila* oocytes about how or when kinetochores interact with microtubule plus ends to achieve bipolar attachment, except the involvement of kinetochore proteins and the chromosomal passenger complex (Radford et al., 2015; Resnick et al., 2009). *sentin* mutants are viable with minimal mitotic defects, but female sterile. In oocytes lacking Sentin, kinetochores and microtubules precociously form robust interactions, leading to frequent attachment of both homologues to the same pole during meiosis I. Therefore, the catastrophe-promoting protein Sentin is responsible for delaying kinetochore-microtubule attachment until spindle bipolarity is fully established in oocytes.

Results and Discussion

sentin mutants are viable and show minimal mitotic defects but are female sterile

To define the role of Sentin in developing flies, we generated four partial deletion mutants of *sentin* by remobilising a P-element inserted in the 5' end of the *sentin* gene (**Fig.S1A**). All alleles were viable but female sterile showing similar defects in mature oocytes (**Fig.S1C**), and we focused our analysis on two alleles (*ΔB* and *Δ19*). Western blots confirmed that full-length Sentin protein was undetectable in both alleles (**Fig.S1B**), and the phenotypes were indistinguishable. Female sterility and the cytological phenotype of *sentin* oocytes were rescued by transgenes expressing a full-length *sentin* cDNA (see below). We did not observe significant defects in somatic mitosis of larval central nervous systems or in male meiosis (**Fig.S1D,E**), suggesting predominantly oocyte-specific roles of Sentin.

Sentin is crucial for separating homologous centromeres apart in oocytes

To identify the role of Sentin in spindle formation in oocytes, *sentin* mutant oocytes were immunostained for α-tubulin and the pole protein Msps or D-TACC. The spindles were bipolar, with Msps and D-TACC accumulated at the poles in most (>75%) mature oocytes that arrest in metaphase I (**Fig.1A**). However, D-TACC accumulation was slightly reduced (**Fig.1B,C**). The spindle was shorter but denser than wild-type control (**Fig.1B,C; Fig.S2A**). Short spindles were observed in Sentin-depleted cultured cells which showed altered microtubule plus end dynamics (Goshima et al., 2007; Li et al., 2011). Chromosomes, including the achiasmatic 4th chromosomes, were more often clustered compactly at the spindle equator sometimes (18%) with protrusions. In contrast, more stretched, individualised chromosomes were observed in control oocytes (**Fig.1B**; **Fig.S2C,D**).

To determine the positions of homologous centromeres, peri-centromeric satellites specific to centromere 3 were visualised by fluorescent *in situ* hybridisation (FISH). In control oocytes, two signals were located at opposite ends of the chromosome mass, representing a

pair of homologous centromeres pulled towards the opposite poles but connected by chromosome arms with chiasmata (**Fig.1D)**. In contrast, homologous centromeres were located closely together (<1 μm) in 45% of the *sentin* mutant oocytes (**Fig.1E**). A probe specific to centromere 2 also showed similar results (**Fig.1E**). The defect was rescued by a transgene expressing a wild-type *sentin* cDNA from the ubiquitin promoter (below), confirming that Sentin is required for separating homologous centromeres.

Taken together, Sentin is a microtubule plus-end regulator crucial for separating homologous centromeres apart in oocytes without an essential role in bipolar spindle formation.

Unseparated homologous centromeres are stably attached to the same pole in *sentin* oocytes

To establish the cause of unseparated homologous centromeres in *sentin* mutants, chromosomes and kinetochores were first visualised in live oocytes using Rcc1-mCherry (Colombié et al., 2013) and GFP-Mis12 (Materials and Methods), respectively. Live imaging preserves dorsal appendages which allow staging of oocytes (**Fig.1A**). In control oocytes, asymmetrically distributed kinetochores were found at an earlier stage (stage 13; **Fig.2A,C**), but were nearly eliminated by a late stage (stage 14; **Fig.2B,C**). In most (>72%) *sentin* mutant oocytes, an unequal number of kinetochores were observed at each end of the chromosome mass at both stages (**Fig.2A-C**) in agreement with the centromere FISH results and immunostaining results (**Fig.S2E**).

To test whether these mis-oriented kinetochores are corrected, we followed these oocytes for another 20 minutes. In all control oocytes, asymmetrically distributed kinetochores in stage 13 changed their positions (**Fig.2A,D**). In contrast, in most (80%) mutant oocytes, asymmetrically distributed kinetochores did not change their positions within the same time frame (**Fig.2A,D**). Therefore, unlike control oocytes, mis-positioned kinetochores are stably maintained in the *sentin* mutant oocytes.

Next, to determine whether and how kinetochores were attached to microtubules, the Rough deal (Rod) protein tagged with GFP (Basto et al, 2004) was used. Rod is part of the RZZ complex, which is continuously recruited to kinetochores and removed by dynein-dependent transport along kinetochore microtubules (Karess, 2005). Therefore, kinetochore microtubules are highlighted by Rod streams, and unattached kinetochores accumulate Rod as foci. In the wild-type control, more than half (55%) of the early stage-13 oocytes had at least one kinetochore which accumulated Rod-GFP (**Fig.2E,G**). At stage 14, no kinetochores accumulated Rod-GFP and Rod-GFP streams were symmetrically moving towards both poles (**Fig.2E; Video 1)**, indicating all homologous kinetochores have achieved bipolar attachments **(**Diagram **i in Fig.2F**).

Unseparated homologous centromeres observed in *sentin* mutant oocytes can be caused by three possibilities, which can be distinguished by the Rod-GFP pattern. Homologous kinetochores either fail to attach microtubules (ii **in Fig.2F**), attach microtubules from opposite poles but failed to be pulled (iii **in Fig.2F)**, or attach microtubules from the same pole (iii in **Fig.2F**). At early stage 13, only a small proportion (20%) of *sentin* mutant oocytes have Rod-GFP accumulated at kinetochores (**Fig.2E,G**), suggesting microtubules may precociously attach to kinetochores. At stage 14, *sentin* mutant oocytes displayed robust Rod-GFP streams, which are often asymmetrical (63% vs 7% in the control), without accumulation at kinetochores (**Fig.2E; Video 2**). This indicates that kinetochores must be robustly attached to microtubules (excluding ii **in Fig.2F**). We did not see Rod-GFP streams emerging from a single point (or two closely located points) in both directions. This excludes the possibility (iii in **Fig.2F**) that unseparated homologous kinetochores are connected to microtubules from the opposite poles. The Rod-GFP pattern in *sentin* mutant oocytes is only consistent with attachment of homologous kinetochores to microtubules from the same pole ("monopolar" or "syntelic" attachment; iv in **Fig.2F**).

In agreement with observations from GFP-Mis12, detachment or direction changes of Rod-GFP streams were rarely observed in stage-14 mutant oocytes even when they were

distributed asymmetrically (one event in a total of 150 minutes of observation). This demonstrates that kinetochore-microtubule attachments are stable in *sentin* mutant oocytes regardless of whether they are attached in a monopolar or bipolar fashion.

Precocious stable kinetochore-microtubule attachments in the *sentin* oocytes

To conclusively define when and how monopolar attachments are established, we followed kinetochore positions from the beginning of spindle formation. In control oocytes, after nuclear envelope break down, spindle microtubules start assembling at roughly around 10 minutes, and spindle bipolarity is established around 30 minutes (Colombié et al., 2008). The start of accumulation of kinetochore proteins (seen by GFP-Mis12 and Rod-GFP) roughly coincides with the start of spindle microtubule assembly (**Fig.3F**). In control oocytes expressing GFP-Mis12, soon after full accumulation of kinetochore proteins (kinetochore maturation), kinetochores dynamically moved from one end of the chromosome mass to the other end, and this dynamic movement persisted even 1 hour after kinetochore maturation (**Fig.3A,B; Video 3**). This persistent dynamic movement in early oocytes has not previously been recognised, because kinetochores had not been visualised in live oocytes before and individual chromosomes could not be resolved. It may be related to previously reported phenomena, such as uncongressed chromosomes (proposed as "prometaphase" figures; Gilliland et al., 2009) or oscillatory movement of achiasmatic chromosomes (Hughes et al., 2009).

In *sentin* oocytes, the behaviour of kinetochores during spindle formation was dramatically different (**Fig.3A,B; Video 4**). In all of the mutant oocytes, kinetochores were much less mobile. Kinetochores usually separated into two (often unequal) groups and migrated to ends of the chromosome mass soon after kinetochore maturation. After they reached the ends, most of the kinetochores rarely changed their positions even when kinetochores were asymmetrically distributed.

To define the timing of kinetochore-microtubule attachments, oocytes expressing Rod-GFP were followed from the beginning of spindle formation (**Fig.3C,D**). In control oocytes, Rod-GFP first accumulated at kinetochores following nuclear envelope break down. Then some kinetochores showed association with a weak stream (arrowheads in **Fig.3C; Video 5**) while Rod-GFP still showed clear accumulation at most kinetochores, indicating weak attachments of microtubules to the kinetochores. Rod-GFP accumulation at most kinetochores persisted well after bipolar spindle formation (**Fig.3C-E**). A delay in end-on kinetochore attachments to microtubules has been reported in mouse oocytes, but has not been previously described in *Drosophila* oocytes.

Remarkably, in *sentin* mutant oocytes, soon after the Rod-GFP accumulated, strong and persistent Rod-GFP streams appeared (**Fig.3D,E; Video 6**). The timing of the appearance of robust Rod-GFP streams was earlier, and the intensity and persistence of the streams were much higher than in control oocytes, although the timings of establishing the spindle bipolarity were comparable (**Fig. S2B**). This demonstrated that robust kinetochore-microtubule attachments were formed precociously in the *sentin* mutant.

To compare microtubule dynamics, we carried out fluorescence recovery after photobleaching (FRAP) of GFP-tubulin in control and *sentin* mutant oocytes. We observed similar recovery at stage 13 and 14 in the control, while *sentin* mutant showed marginally slower recovery at stage 13 as compared with stage 14 (**Fig. S3**). It remains to be seen whether this difference, if any, represents a change in microtubule dynamics.

Sentin is enriched at acentrosomal spindle poles in oocytes after establishment of the bipolar spindle

In S2 cells, Sentin is recruited to microtubule plus ends by EB1 through direct physical interaction. During mitosis, EB1 and Sentin colocalise all over the spindle as moving comets. To determine the localisation of Sentin on meiotic spindles in oocytes, mature stage-14 control wild-type oocytes were immunostained with Sentin and α-tubulin antibodies.

Interestingly Sentin was accumulated at poles of meiotic spindles in most (68%) oocytes (**Fig.4A**). The signal was lost in the *sentin* mutant (**Fig.4A**), confirming this represents endogenous localisation of the Sentin protein. Co-staining of Sentin and EB1 highlighted uniform localisation of EB1 all over meiotic spindles in all oocytes, in clear contrast with the mostly pole accumulation of Sentin (**Fig.4B**).

To follow Sentin localisation through different stages, transgenic flies expressing GFP-tagged Sentin under the control of a ubiquitin promoter were generated, although we cannot exclude the possibility that it may not accurately reflect the endogenous localisation. GFP-Sentin localised all over the spindle in most (23%) oocytes at early stage 13, while by stage 14 it accumulated at the spindle poles in all oocytes (**Fig.4C**). To confirm this observation, we observed the oocytes expressing GFP-Sentin from nuclear envelope breakdown. GFP-Sentin localised all over the spindle at early stages when spindle bipolarity has not been established. In the same oocytes, GFP-Sentin has subsequently accumulated only well after spindle bipolarity is established (**Fig.4D**). Early Sentin localisation all over the spindle may contribute to the instability of microtubule-kinetochore attachments, while late sequestration of Sentin at the poles may contribute to more stable attachments after establishment of a bipolar spindle.

To understand relationships between the localisation, function and EB1 interaction, we first expressed GFP-tagged full-length Sentin and Sentin(1-840) lacking the EB1 interaction domain (Li et al., 2011) in control oocytes. In both cases, they accumulated to the spindle poles in mature oocytes (**Fig.4E**), indicating that EB1 interaction is not required for Sentin pole localisation. Next, to test whether EB1 interaction is required for the Sentin function, Sentin(1-840) lacking the EB1-interaction domain was expressed in the *sentin* mutant. A full-length Sentin rescued the *sentin* defect, while Sentin(1-840) under the same promoter failed to rescue it (**Fig.4F**). Immunoblotting confirmed that proteins with the predicted sizes were expressed (**Fig.4G**). These results showed that EB1 interaction is essential for Sentin function, but not its pole localisation, supporting a hypothesis that Sentin

functions at microtubule ends, and late localisation to the spindle pole may help to stabilise kinetochore-microtubule attachments.

Sentin-EB1 prevents precocious kinetochore attachments to facilitate bipolar attachments of bivalent chromosomes in oocytes

In this report, we showed that *Drosophila* oocytes delay robust end-on attachments of microtubules to kinetochores. Similar delay is also observed in mouse oocytes (Brunet et al., 1999; Kitajima et al., 2011), demonstrating that this is a widely conserved phenomenon in oocytes. This long delay is oocyte-specific, and is not seen in mitotic cells. As establishment of spindle bipolarity takes much longer in oocytes due to a lack of centrosomes, this oocyte-specific long delay is likely to help kinetochores not to form robust microtubule attachments before a bipolar spindle is fully established. We found that the EB1-interacting protein Sentin is responsible for preventing microtubules from precociously forming robust attachments to kinetochores (**Fig.4H**).

We have previously shown *in vitro* that Sentin, through physical interaction with EB1, directly increases growth and catastrophe rates of microtubule plus ends, and also recruits Msps, the XMAP215 orthologue, to increase the microtubule growth and rescue rates (Li et al., 2012). In this study, we showed that the role of Sentin to destabilise kinetochore-microtubule attachments requires the interaction with EB1. A female sterile *msps* mutant does not have a *sentin*-like defect (Cullen and Ohkura, 2001), suggesting the catastrophe-promoting activity of Sentin-EB1 is key to destabilising the attachments.

sentin mutant oocytes have a high frequency of homologous centromeres attached to the same pole even at later stages. Live imaging showed that incorrect attachments remain stable and uncorrected. Observation in activated oocytes showed chromosome mis-segregation in 4 out of 5 anaphase I, which explains most of the infertility. We are not sure at the moment whether Sentin specifically destabilises incorrect attachments or indiscriminately destabilises all attachments. In mouse oocytes, persistent Aurora B/C at kinetochores

destabilises both correct and incorrect attachments, and later recruitment of the phosphatase PP2A-B56 to kinetochores stabilises the attachments (Yoshida et al., 2015). Also in *Drosophila* oocytes, the Aurora B activity is required for normal bi-orientation of homologous centromeres (Resnick et al, 2009), but did not appear to be compromised in the *sentin* mutant (**Fig.S2F-H**). We found in *Drosophila* oocytes that Sentin accumulates at spindle poles well after establishment of spindle bipolarity independently of its EB1 interaction. This late pole localisation which sequesters the catastrophe factor away from kinetochores may be one of the mechanisms to stabilise kinetochore-microtubule attachments after the establishment of spindle bipolarity.

Taken together, Sentin with microtubule catastrophe-promoting activity facilitates bipolar attachment of homologous chromosomes in oocytes by destabilising the kinetochore-microtubule attachments during acentrosomal spindle formation. Previously in mouse oocytes, phospho-regulation of kinetochore proteins is shown to be responsible for the delay in forming stable kinetochore-microtubule attachments (Yoshida et al., 2015). Our finding in *Drosophila* oocytes demonstrates that regulation of microtubule plus ends is a novel mechanism to delay stable attachments. It is possible that *Drosophila* and mouse use different mechanisms to achieve the same goal, but also possible that both organisms use these two mechanisms in parallel with different contributions.

Materials and Methods

Fly genetics

Genes, mutations and chromosome aberrations are described in Flybase (Drysdale et al., 2008) and Lindsley and Zimm (1992). Standard fly techniques were used (Ashburner et al., 2005). For generation of *sentin* mutants, chromosomes in progeny of jump starter males carrying both *Δ2-3* and the P-element *EY00443* were selected for a loss of w^+. The regions of deletions were determined by PCR and sequencing from the mutant genomic DNA. For rescue of *sentin* mutants by a transgene, a single copy of a transgene was introduced in flies carrying *sentinΔB* mutation over a deficiency and at least two independent insertions were tested. In most cases, the phenotype of *sentin* mutants were observed over a deficiency uncovering *sentin* (*Df(3R)ED4515* or *Df(3R)BSC737*), and a homozygous wild-type allele or a wild-type allele over a *sentin* mutation with matched transgene combinations were used as a wild-type control.

The frequency of sex chromosome non-disjunction in males was measured according to Meireles et al. (2009). For live imaging, *GFP-Mis12* and *Rcc1-mCherry* under *UASp* was driven by *nos-GAL4* (*MVD1*) and Rod-GFP is controlled under its own promoter (a kind gift from R. Karess; Basto et al., 2004). All transgenes and *sentin* mutations are located on the third chromosomes and recombined together on the same chromosome when necessary. These recombined chromosomes were observed over a *sentin* deficiency (*sentin* mutant) or wild-type chromosome (control). In some cases, an equivalent recombinant chromosome without a *sentin* mutation over wild-type chromosome was used as a control.

Molecular work

Standard molecular techniques (Sambrook et al, 1989) were used. For *sentin* transgenes, the coding region of the full-length *sentin* or part of *sentin* corresponding 1-840 residues were cloned into a Gateway vector modified from pWR-Ubq (generated by N.Brown's lab). *GFP-*

Mis12 under the *UASp* promoter was generated using pPGW Gateway vector (generated by T. Murphy's lab). Transgenic flies were generated by Genetic Service Inc using P-element mediated transformation. Protein samples for western blots were prepared by homogenising whole adult females after heat-treatment at 98°C.

Antibodies used for western blotting were mouse anti-α-tubulin (DM1A; Sigma), rabbit anti-Sentin (Li et al., 2011) and peroxidase conjugated secondary antibodies (Jackson), and detected by ECL (GE Healthcare). To generate the rat anti-Sentin antibody, the insoluble fraction of BL21/pLysS expressing MBP-Sentin was run on SDS gel and MBP-Sentin was extracted from the gel and used to immunise two rats by the Scottish Blood Transfusion Service.

Cytological study

For live imaging, ovaries were dissected in halocarbon oil (700; Halocarbon) from adult females matured for 4-7 days at 18°C. The morphology of dorsal appendages was used to determine the stage of oocytes. Oocytes were observed at room temperature under a microscope (Axiovert; Carl Zeiss) attached to a spinning-disk confocal head (Yokogawa) controlled by Volocity (PerkinElmer). Z-slices with a 0.8 μm interval were captured every half minute or minute, and are presented after maximum intensity projection onto the XY plane. To generate kymographs using Volocity, a 3D image of each time point was first projected onto the XY plane, and this 2D image was then projected onto the long axis of the spindle using maximum intensity projection. This compressed 1D image was aligned against time. Fisher's exact test and t-test were used for categorical and parametrical data, respectively.

The strength of kinetochore attachment to microtubules was classified into four levels using Rod-GFP patterns by the following criteria: 1) no visible Rod-GFP stream with clear accumulation on the kinetochore was classified as no attachment, 2) a faint stream with clear accumulation on the kinetochore was classified as weak attachment, 3) a clear stream with significantly less intensity than the signal at the kinetochore was classified as moderate

attachment, 4) a clear stream as strong as the kinetochore signal was classified as strong attachment.

FRAP was carried out and analysed as previously described (Colombie et al., 2013) with the following modifications. The rectangular box (12 μm X 8.5 μm) covering a half-spindle was bleached using 25 iterations of the 488 nm laser at 100% power, and three Z-slices were taken at 1 μm interval every 5 seconds. After maximum intensity projection, the total signal intensity of a 1x1 μm square within the bleached area on the spindle was measured. The signal intensity was normalised so that the pre-bleached value is one and the value at the first time point after bleaching is zero.

Mitosis was analysed after the aceto-orcein staining of squashed larval central nervous systems as described in Cullen et al. (1999). Post-meiotic figures in testes were analysed by phase contrast microscopy after gentle squashing as described in Bonaccorsi et al. (2000). Oocytes were immunostained after methanol fixation as described in Cullen et al. (2001). FISH of oocytes was carried out according to Meireles et al (2009) and Loh et al. (2012). Immunostaining and FISH in oocytes were carried out after the maturation of young adults for 3-5 days at 25°C or for 4-7 days at 18°C. Under these conditions, most fully grown oocytes were arrested at stage 14 and generally considered as mature stage-14 oocytes for our immunostaining, as there is no accurate staging methods due to loss of dorsal appendages. Immunostained oocytes were examined using a PlanApochromat objective lens (63X NA1.4) on LSM5.10 Exciter (Zeiss) unless stated otherwise, and images were presented after maximum intensity projection onto the XY plane. To take higher resolution images (Fig. S2E), mature oocytes were fixed in formaldehyde/heptane and stained with Hoechst 33342, and images were taken on an SP5 (Leica) with 63x 1.4 NA lens (the pixel size of 53.4 nm) as previously described (Radford et al 2012). Activated oocytes were collected every 10 minutes and fixed in methanol for immunostaining to observe anaphase I and later stages. Chromosome mis-segregation in meiosis I was estimated by unequal numbers of segregated chromosomes. Antibodies used were mouse anti-α-tubulin (1/250;

DM1A; Sigma), rabbit anti-EB1 (1/500; HN285; Elliott et al, 2005), rabbit anti-Sentin (1/1000; Li et al., 2011), rabbit anti-Msps (1/100; HN264; Cullen and Ohkura, 2001), rabbit anti-D-TACC-CTD (1/1000; Loh et al, 2012) and secondary antibodies conjugated with Cy3 or Alexa488 fluorescent dyes (Jackson or Molecular Probes). DNA was stained with 0.4 µg/ml of DAPI (Sigma). For a pericentromeric satellite specific to the second chromosome, a synthetic oligonucleotide $(aacac)_6$ was used as a probe.

Online supplemental materials

Fig. S1 shows generation of *sentin* mutants and their phenotypes. Fig. S2 shows detailed phenotypes of *sentin* mutant oocytes including evidence for unaltered Aurora B activity and localisation. Fig. S3 presents FRAP analysis of GFP-α-tubulin in control and *sentin* mutant oocytes. Videos show wild-type and *sentin* stage-14 oocyte expressing Rod-GFP Rcc1-mCherry (Video 1, Video 2), wild-type and *sentin* stage-13 oocyte expressing GFP-Mis12 Rcc1-mCherry (Video 3, Video 4) and wild-type and *sentin* stage-13 oocyte expressing Rod-GFP Rcc1-mCherry (Video 5, Video 6).

Acknowledgements

We thank R. Karess, Bloomington Drosophila Stock Center (NIH P40OD018537) and Resource Center (NIH 2P40OD010949-10A1), and *Drosophila* gene disruption project for providing reagents and fly stocks. We specially thank A. Satoh for helping mutant generation, S. Beard and H. Grey for generating antibodies, T. Maresca for an Ndc80 antibody, R. Beaven for critical reading of the manuscript and members of McKim and Ohkura labs for discussion. The authors declare no competing financial interests. The works in Goshima, Ohkura and McKim labs are supported by Grants-in-Aid for Scientific Research (15H01317, MEXT), the Wellcome Trust (081849, 086574, 092076, 098030, 099827) and NIH (GM10955), respectively.

References

Ashburner, M., K.G. Golic, and R.S. Hawley. 2005. *Drosophila*: A Laboratory Handbook. Cold Spring Harbor Laboratory Press, Cold Spring Harbor, NY. 1409 pp.

Basto, R., F. Scaerou, S. Mische, E. Wojcik, C. Lefebvre, R. Gomes, T. Hays, and R. Karess. 2004. In vivo dynamics of the rough deal checkpoint protein during *Drosophila* mitosis. *Curr Biol.* 14:56-61.

Bonaccorsi, S., M.G. Giansanti, G. Cenci, and M. Gatti. 2000. Cytological analysis of spermatocyte growth and male meiosis in *Drosophila melanogaster*. In *Drosophila* Protocols. W. Sullivan, M. Ashburner, R. Scott Hawley, editors. Cold Spring Harbor Laboratory Press, Cold Spring Harbor, NY. 87–109.

Brunet, S., A.S. Maria, P. Guillaud, D. Dujardin, J.Z. Kubiak, and B. Maro. 1999. Kinetochore fibers are not involved in the formation of the first meiotic spindle in mouse oocytes, but control the exit from the first meiotic M phase. *J. Cell Biol.* 146:1-12.

Cheeseman, I.M. 2014. The kinetochore. *Cold Spring Harb Perspect Biol.* 6:a015826.

Colombie, N., C. F. Cullen, A. L. Brittle, J. K. Jang, W. C. Earnshaw, M. Carmena, K. McKim, and H. Ohkura. 2008. Dual roles of Incenp crucial to the assembly of the acentrosomal metaphase spindle in female meiosis. *Development* 135:3239-3246.

Colombie, N., A.A. Gluszek, A.M. Meireles, and H. Ohkura. 2013. Meiosis-specific stable binding of Augmin to acentrosomal spindle poles promotes biased microtubule assembly in oocytes. *PLoS Genet.* 6:e1003562.

Cullen, C.F., P. Deak, D.M. Glover, and H. Ohkura. 1999. *mini spindles*: a gene encoding a conserved microtubule associated protein required for the integrity of the mitotic spindle in *Drosophila*. *J. Cell Biol*. 146:1005-1018.

Cullen, C.F. and H. Ohkura. 2001. Msps protein is localised to acentrosomal poles to ensure the bipolarity of *Drosophila* meiotic spindles. *Nature Cell Biol.* 3:637-642.

Davydenko, O., R.M. Schultz, and M.A. Lampson. 2013. Increased CDK1 activity determines the timing of kinetochore-microtubule attachments in meiosis I. *J Cell Biol.* 202:221-229.

Drysdale R; FlyBase Consortium. 2008. FlyBase: a database for the *Drosophila* research community. *Methods Mol. Biol.* 420:45-59.

Elliott, S.L., C.F. Cullen, N. Wrobel, M.J. Kernan, and H. Ohkura. 2005. EB1 is essential during *Drosophila* development and plays a crucial role in the integrity of chordotonal mechanosensory organs. *Mol. Biol. Cell.* 16:891-901.

Gilliland, W.D., S.F. Hughes, D.R. Vietti, and R.S. Hawley. 2009. Congression of achiasmate chromosomes to the metaphase plate in *Drosophila melanogaster* oocytes. *Dev. Biol.* 325:122-128.

Goshima, G., R. Wollman, S.S. Goodwin, N. Zhang, J.M. Scholey, R.D, Vale, and N. Stuurman. 2007. Genes required for mitotic spindle assembly in *Drosophila* S2 cells. *Science.* 316:417-421.

Hughes, S.E., W.D. Gilliland, J.L. Cotitta, S. Takeo, K.A. Collins, and R.S. Hawley. 2009. Heterochromatic threads connect oscillating chromosomes during prometaphase I in *Drosophila* oocytes. *PLoS Genet.* 5:e1000348.

Karess, R. 2005. Rod-Zw10-Zwilch: a key player in the spindle checkpoint. *Trends Cell Biol.* 15:386-392.

Kitajima, T.S., M. Ohsugi, and J. Ellenberg. 2011. Complete kinetochore tracking reveals error-prone homologous chromosome biorientation in mammalian oocytes. *Cell.* 146:568-581.

Li, W., T. Miki, T. Watanabe, M. Kakeno, I. Sugiyama, K. Kaibuchi, and G. Goshima. 2011. EB1 promotes microtubule dynamics by recruiting Sentin in *Drosophila* cells. *J. Cell Biol.* 193:973-983.

Li, W., T. Moriwaki, T. Tani, T. Watanabe, K. Kaibuchi, and G. Goshima. 2012. Reconstitution of dynamic microtubules with *Drosophila* XMAP215, EB1, and Sentin. *J. Cell Biol.* 199:849-862.

Lindsley, D.L. and G.G. Zimm. 1992. The Genome of *Drosophila melanogaster*. Academic Press, New York. 1133 pp.

Loh, B.J., C.F. Cullen, N. Vogt, and H. Ohkura. 2012. The conserved kinase SRPK regulates karyosome formation and spindle microtubule assembly in *Drosophila* oocytes. *J. Cell Sci.* 125:4457-4462.

Meireles, A.M., K.H. Fisher, N. Colombie, J.G. Wakefield, and H. Ohkura. 2009. Wac: a new Augmin subunit required for chromosome alignment but not for acentrosomal microtubule assembly in female meiosis. *J. Cell Biol.* 184:777-784.

Radford, S.J., A.M. Harrison, and K.S. McKim. 2012. Microtubule-depolymerizing kinesin KLP10A restricts the length of the acentrosomal meiotic spindle in *Drosophila* females. Genetics. 192:431-440.

Radford, S.J., T.L. Hoang, A.A. Głuszek, H. Ohkura, and K.S. McKim. 2015. Lateral and end-on kinetochore attachments are coordinated to achieve bi-orientation in *Drosophila* oocytes. *PLoS Genet.* 11:e1005605.

Resnick, T.D., K.J. Dej, Y. Xiang, R.S. Hawley, C. Ahn, T.L. Orr-Weaver. 2009. Mutations in the chromosomal passenger complex and the condensin complex differentially affect synaptonemal complex disassembly and metaphase I configuration in Drosophila female meiosis. *Genetics*. 181:875-887.

Sambrook, J., E.F. Fritsch, and T. Maniatis. 1989. Molecular Cloning: A Laboratory Manual. Cold Spring Harbor Laboratory Press, Cold Spring Harbor, NY. 1751 pp.

van der Vaart, B., C. Manatschal, I. Grigoriev, V. Olieric, S.M. Gouveia, S. Bjelic, J. Demmers, I. Vorobjev, C.C. Hoogenraad, M.O. Steinmetz, A. Akhmanova. 2011. SLAIN2 links microtubule plus end-tracking proteins and controls microtubule growth in interphase. *J. Cell Biol*. 193:1083–1099.

Yoshida, S., M. Kaido, and T.S. Kitajima. 2015. Inherent instability of correct kinetochore-microtubule attachments during meiosis I in oocytes. *Dev. Cell.* 33:589-602.

Figure legends

Figure 1. Sentin is required to separate homologous centromeres in oocytes

(A) Meiotic progression in *Drosophila* oocytes. (B) Immunostaining of mature oocytes. (C) Frequency of Msps and D-TACC concentrated at the spindle poles, and bipolar spindles in wild-type (control) and *sentin* mature oocytes (n=13,36,24,58,95,66). The error bars of the spindle length indicate the standard error of the mean (n=94,120). Other error bars indicate the 95% confidence intervals. ** and *** indicate significant differences between wild type and *sentin* ($p<0.01$ and <0.001 respectively). (D) FISH in oocytes using a dodeca-satellite probe specific to centromere 3. (E) The distances between homologous centromeres from FISH probed by dodeca satellite (cen 3) and AACAC satellite repeat (cen 2). ** and *** indicate significant differences from the medians of wild-type control ($p<0.01$ and <0.001 respectively). Scale bars=10 μm.

Figure 2. Monopolar attachment of homologous kinetochores in *sentin* oocytes

(A) Live stage-13 oocytes expressing GFP-Mis12 and Rcc1-mCherry. (B) Stage-14 oocytes expressing GFP-Mis12 and Rcc1-mCherry. (C) The frequency of asymmetric kinetochore distributions seen by GFP-Mis12 (n=26,11,31,29). (D) The frequencies of position change of asymmetrically distributed kinetochores within 20 minutes, seen by GFP-Mis12 (n=5,10,0,12). ND; Not done due to no control stage-14 oocytes with asymmetrically distributed kinetochores observable for 20 minutes. (E) Live mature oocytes expressing GFP-Rod and Rcc1-mCherry. Arrowheads point to accumulated Rod-GFP. (F) Diagrams of various attachment modes with expected Rod-GFP localisation. Only monopolar attachments can explain the unseparated homologous centromeres observed in *sentin* mutant oocytes. (G) The frequency of oocytes with at least one kinetochore accumulating Rod-GFP (n=25,20,10,12,18,21). *, ** and *** indicate significant differences from the control ($p<0.05$, 0.01, 0.001). Error bars indicate the 95% confidence intervals. Scale bars=10 μm.

Figure 3. Sentin suppresses precocious stable kinetochore-microtubule attachments

(A) Time lapse images of oocytes expressing GFP-Mis12 and Rcc1-mCherry. The numbers are in minutes from full recruitment of Mis12. (B) Kymographs of the same oocytes with the long axis of the spindle against time (the Y-axis). (C) Time lapse images of oocytes expressing Rod-GFP and Rcc1-mCherry. The numbers are in minutes from full recruitment of Rod. Arrowheads indicate Rod-GFP streams. (D) Kymographs of the same oocytes. (E) The frequency of weakly (open bars), moderately (half filled) and strongly (filled) attached kinetochores judged by Rod-GFP (Materials and Methods). For each genotype, a total of 20-32 kinetochores in 5 oocytes were followed. * and *** indicate significant differences from the control ($p<0.05$ and <0.001, respectively). Error bars indicate the 95% confidence intervals of the proportion of attached kinetochores. (F) The approximate timing of cytological events in oocytes. Time 0 is defined as the time when full recruitment of kinetochore proteins, Mis12 and Rod, has occurred. Nuclear envelope breakdown (NEB), kinetochore (KT), microtubule (MT). Scale bars=10 μm.

Figure 4. Sentin function, not pole localisation, depends on EB1 interaction

(A,B) Immunostaining of mature oocytes. (C) Localisation of GFP-Sentin at different stages of oocytes (n=13,5,12). Error bars indicate the 95% confidence intervals. (D) Time lapse images of oocytes expressing GFP-Sentin and Rcc1-mCherry. The numbers indicate minutes from NEB. (E) Live wild-type control oocyte expressing GFP-tagged full-length Sentin and Sentin (1-840) lacking the EB1-interacting domain. (F) The distances between homologous centromeres (cen 3) in mature oocytes from wild-type control and *sentin* mutants without a transgene (–) and with transgenes expressing full-length Sentin and Sentin(1-840). *** indicates a significant difference from the control ($p<0.001$). (G) Immunoblots of adult females from strains shown in F probed with antibodies against Sentin (upper) and α-tubulin (lower). (H) A model of Sentin action. Scale bars=10 μm.

Supplementary Figure Legends

Figure S1. *sentin* mutants are viable but female sterile

(A) The genomic region around *sentin* in wild type, *sentin* mutants (*Δ19, ΔB*) and their parental line with a P-element insertion (triangle). (B) Western blots of adult females for Sentin and α-tubulin. (C) The distances between homologous centromeres from FISH probed by dodeca satellite (cen 3). *** indicates a significant difference from the medians of wild-type control ($p<0.001$). (D) Mitotic index and % of anaphase among mitosis in central nervous systems of wild-type control and *sentin* mutant larvae (n=5,4). (E) Nuclear diameter of spermatids at onion stage and mis-segregation rate of sex chromosomes in male meiosis (n=59, 213, 1451, 434). Error bars indicate the standard error of the mean (left) and 95% confidence intervals (right).

Figure S2. The phenotype of *sentin* mutant oocytes with unaltered Aurora B activity and localisation

(A) Microtubule density estimated by the maximum tubulin signal intensity of the spindle in fixed stage 14 oocytes. n=56, 64. Error bars represent standard error of the mean. (B) Time taken from kinetochore maturation (full recruitment of Rod-GFP) to establishment of the spindle bipolarity in live oocytes expressing Rod-GFP and Rcc1-mCherry. Rod-GFP streams were used to estimate the timing of establishment of spindle bipolarity, which was consistent with the timing from live imaging using GFP-tubulin. n=5. Error bars represent standard error of the mean. (C) The proportion of DAPI-stained mature oocytes in which at least one chromosome can be recognised separately from others. n=59, 51. (D) The proportion of DAPI-stained mature oocytes with the following location of the two 4th chromosomes (represented by small dots). From left to right; both are located together with the other chromosomes; only one is located closer to the poles and separated from the other chromosomes; each of the two is located closer to the opposite pole and separated from the

other chromosomes; both are located closer to the same pole and separated from the chromosome mass. n=58, 41. All error bars in C and D represent 95% confidence intervals. *** indicates a significant difference from the control ($p<0.001$). (E) High magnification images of the meiotic spindle in mature oocytes from wild-type control and *sentin*$^{32/Df}$ mutant. The inserts (scale bars=1 μm) are magnified images of the areas indicated in the boxes. (F) Wild-type control and *sentin* mature oocytes expressing GFP-Incenp and Rcc1-mCherry driven by *nanos-GAL4*. GFP-Incenp localisation to the spindle equator and centromeres was not affected by the *sentin* mutation. (G) Immunostaining images of phospho-H3-Ser10 (H3P), α-tubulin and DNA in control and *sentin* mature oocytes. The maximum intensities of H3-P signals were measured. No significant difference was observed. Error bars represent standard error of the mean. (H) Wild-type control, *sentin* and *incenp*^{QA26} mature oocytes expressing Rod-GFP and Rcc1-mCherry. The proportion of robust Rod-GFP localisation in oocytes was shown with each genotype. The results showed that full Rod recruitment requires the Aurora B activity as shown in mammalian mitotic cells, but is not affected in the *sentin* mutant, implying that Aurora B activity is not compromised in *sentin* mutant oocytes. The error bars represent 95% confidence intervals. *** indicates $p<0.001$. n=18, 21, 30. Scale bars=10 μm.

Figure S3. FRAP analysis of GFP-α-tubulin in control and *sentin* mutant oocytes

Oocytes at stage 13 and 14 expressing GFP-α-tubulin and Rcc1-mCherry driven by n*anos-GAL4* were used. GFP-tubulin of a half spindle was photobleached and the recovery was followed. (A) Raw intensity values are plotted against time. GFP-tubulin intensity in the *senitn* mutant is higher than the control, consistent with immunostaining results. (B) The signal intensity was normalised so that one corresponds to the pre-bleached value and zero corresponds to the value at the first time point after bleaching. n=21-27. Error bars represent the standard error of the mean. * indicates a significant difference between the two stages of *sentin* ($p<0.05$; one-tail t-test).

Supplementary Video information

Video 1. Wild-type stage-14 oocyte expressing Rod-GFP Rcc1-mCherry (20 µm x 15 µm x 20 min)

Video 2. *sentin* stage-14 oocytes expressing Rod-GFP Rcc1-mCherry (15 µm x 20 µm x 20 min)

Video 3. Wild-type stage-13 oocyte expressing GFP-Mis12 Rcc1-mCherry (18 µm x 18 µm x 90 min)

Video 4. *sentin* stage-13 oocyte expressing GFP-Mis12 Rcc1-mCherry (18 µm x 18 µm x 90 min)

Video 5. Wild-type stage-13 oocyte expressing Rod-GFP Rcc1-mCherry (25 µm x 25 µm x 60 min)

Video 6. *sentin* stage-13 oocyte expressing Rod-GFP Rcc1-mCherry (25 µm x 25 µm x 60 min)

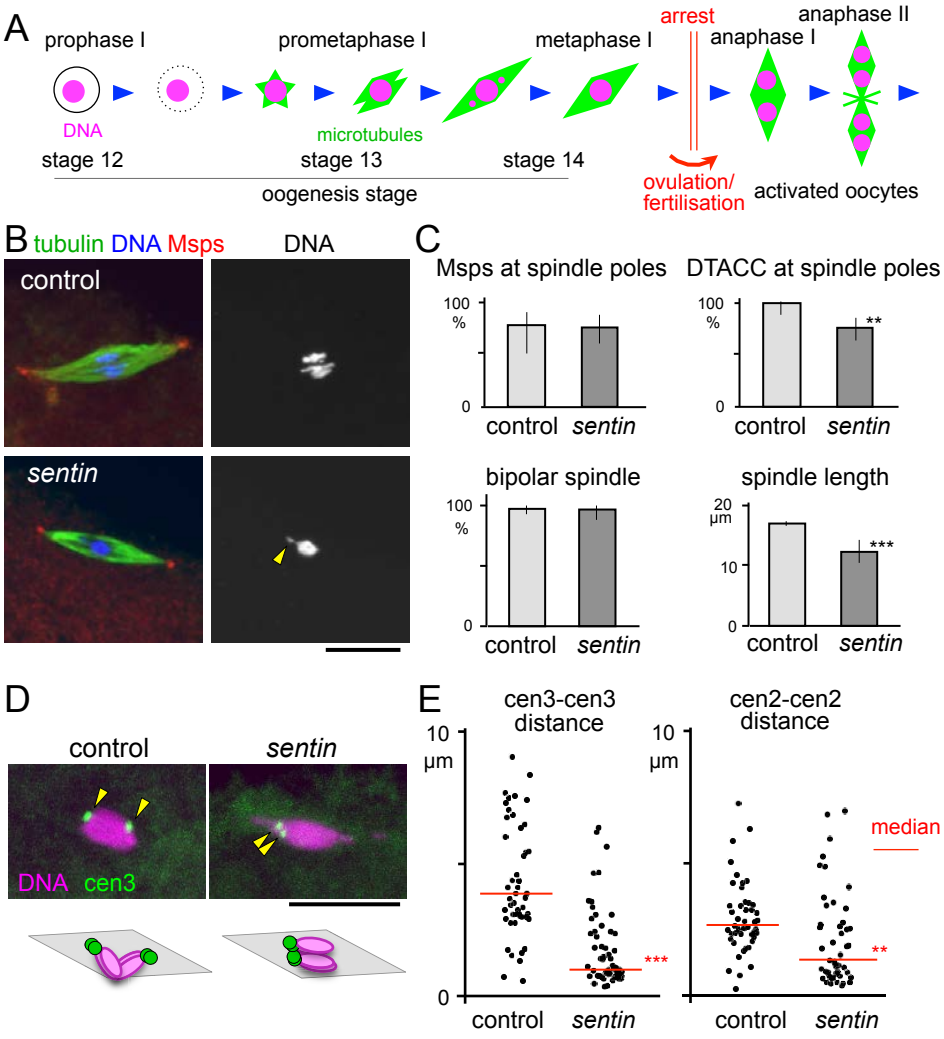
A
prophase I
prometaphase I
metaphase I
arrest
anaphase I
anaphase II
DNA
microtubules
stage 12
stage 13
stage 14
oogenesis stage
ovulation/
fertilisation
activated oocytes
B tubulin DNA Msps
DNA
control
sentin
C
Msps at spindle poles
DTACC at spindle poles
100 %
0
control
sentin
**
bipolar spindle
spindle length
20 µm
10
***
D
control
sentin
DNA cen3
E
cen3-cen3 distance
cen2-cen2 distance
10 µm
0
median

Figure 1

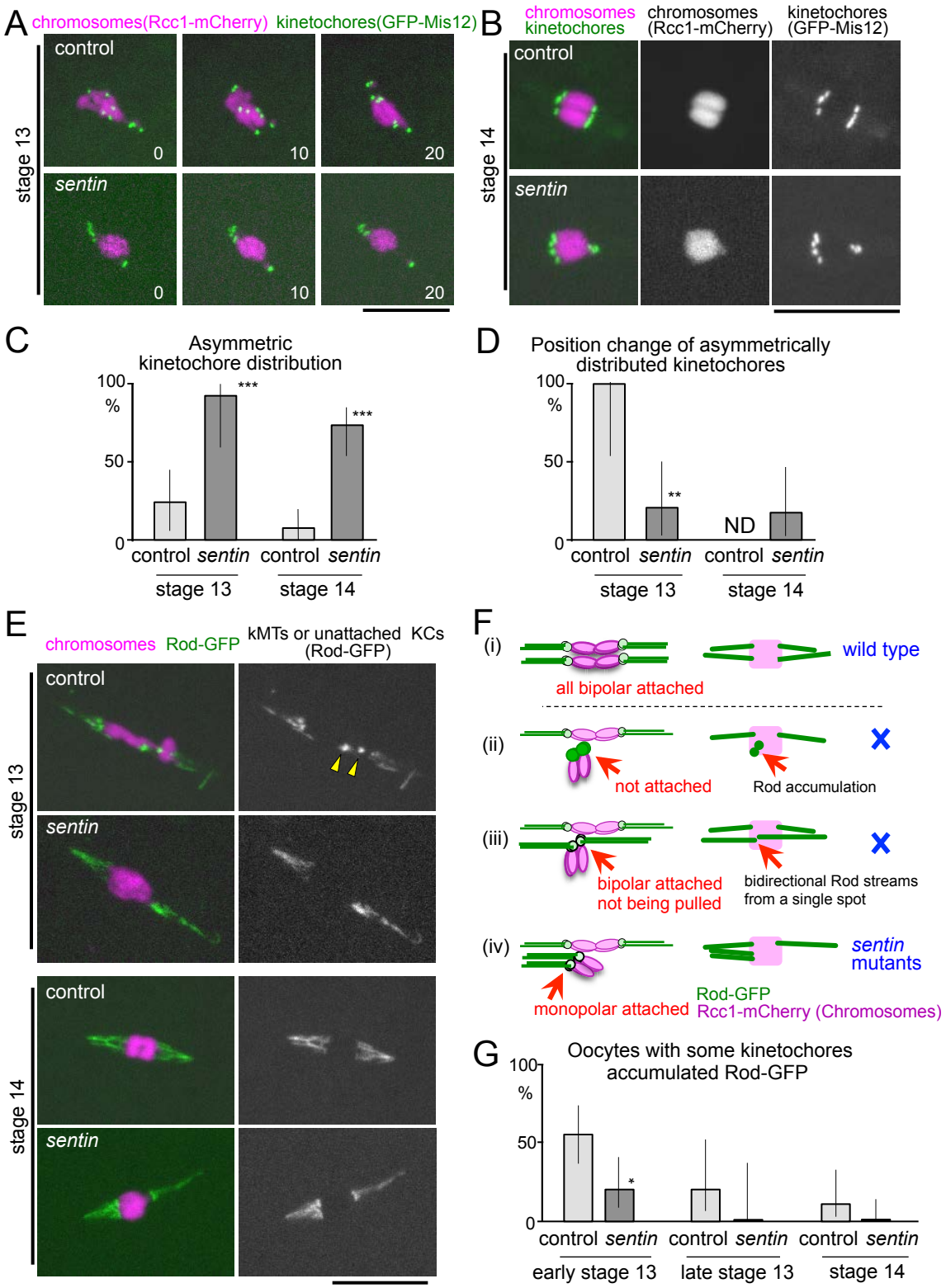
A
chromosomes(Rcc1-mCherry)
kinetochores(GFP-Mis12)
control
sentin
stage 13
0
10
20
B
chromosomes
kinetochores
chromosomes
(Rcc1-mCherry)
kinetochores
(GFP-Mis12)
control
sentin
stage 14
C
Asymmetric
kinetochore distribution
100
%
50
0
***
***
control
sentin
control
sentin
stage 13
stage 14
D
Position change of asymmetrically
distributed kinetochores
100
%
50
0
**
ND
control
sentin
control
sentin
stage 13
stage 14
E
chromosomes
Rod-GFP
kMTs or unattached KCs
(Rod-GFP)
control
sentin
control
sentin
stage 13
stage 14
F
(i)
wild type
all bipolar attached
(ii)
not attached
Rod accumulation
(iii)
bipolar attached
not being pulled
bidirectional Rod streams
from a single spot
(iv)
sentin
mutants
monopolar attached
Rod-GFP
Rcc1-mCherry (Chromosomes)
G
Oocytes with some kinetochores
accumulated Rod-GFP
100
%
50
0
*
control
sentin
control
sentin
control
sentin
early stage 13
late stage 13
stage 14

Figure 2

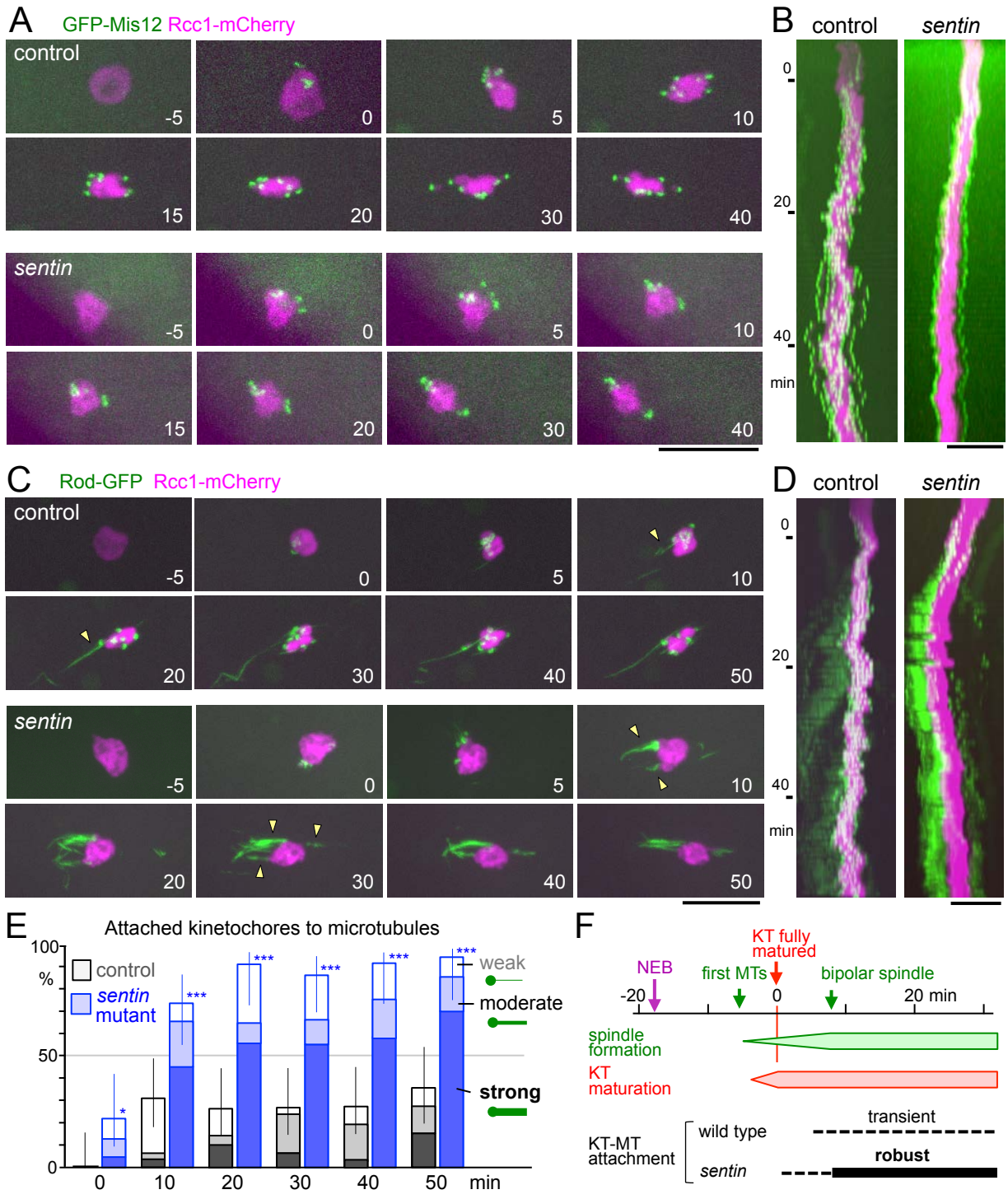
A
GFP-Mis12 Rcc1-mCherry
control
sentin
-5
0
5
10
15
20
30
40
B
control
sentin
0
20
40
min
C
Rod-GFP Rcc1-mCherry
control
sentin
-5
0
5
10
20
30
40
50
D
control
sentin
0
20
40
min
E
Attached kinetochores to microtubules
100
%
50
0
control
sentin
mutant
weak
moderate
strong
***
*
0
10
20
30
40
50
min
F
KT fully
matured
NEB
first MTs
bipolar spindle
-20
0
20 min
spindle
formation
KT
maturation
KT-MT
attachment
wild type
sentin
transient
robust

Figure 3

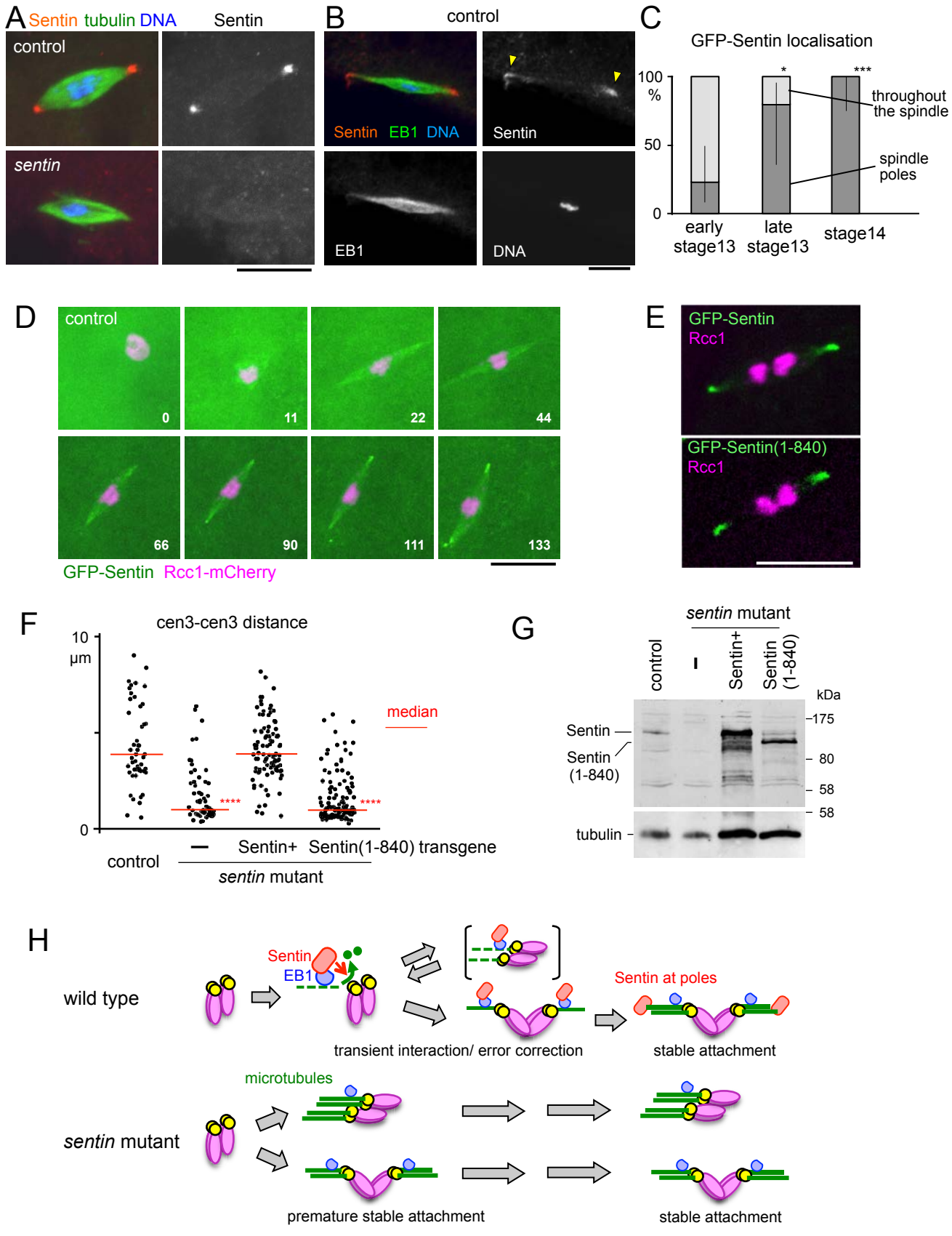
A
Sentin tubulin DNA
Sentin
control
sentin
B
control
Sentin EB1 DNA
Sentin
EB1
DNA
C
GFP-Sentin localisation
100 %
50
0
*
***
throughout the spindle
spindle poles
early stage13
late stage13
stage14
D
control
0
11
22
44
66
90
111
133
GFP-Sentin Rcc1-mCherry
E
GFP-Sentin
Rcc1
GFP-Sentin(1-840)
Rcc1
F
cen3-cen3 distance
10 µm
0
median
****
****
control
—
Sentin+
Sentin(1-840) transgene
sentin mutant
G
sentin mutant
control
—
Sentin+
Sentin (1-840)
kDa
Sentin
Sentin (1-840)
175
80
58
58
tubulin
H
wild type
Sentin
EB1
transient interaction/ error correction
Sentin at poles
stable attachment
microtubules
sentin mutant
premature stable attachment
stable attachment

Figure 4